

Data-Driven Successive Linearization for Optimal Voltage Control

Yiwei Dong, Wenqi Cui, Han Xu, Adam Wierman, Steven Low

Abstract—Power distribution systems are increasingly exposed to large voltage fluctuations driven by intermittent solar photovoltaic generation and rapidly varying loads (e.g., electric vehicles and storage). To address this challenge, a number of advanced controllers have been proposed for voltage regulation. However, these controllers typically rely on fixed linear approximations of voltage dynamics. As a result, the solutions may become infeasible when applied to the actual voltage behavior governed by nonlinear power flow equations, particularly under heavy power injection from distributed energy resources. This paper proposes a data-driven successive linearization approach for voltage control under nonlinear power flow constraints. By leveraging the fact that the deviation between the nonlinear power flow solution and its linearization is bounded by the distance from the operating point, we perform data-driven linearization around the most recent operating point. Convergence of the proposed method to a neighborhood of KKT points is established by exploiting the convexity of the objective function and the structural properties of the nonlinear constraints. Case studies show that the proposed approach achieves fast convergence and adapts quickly to changes in net load.

I. INTRODUCTION

Power distribution systems need to maintain voltage within 5%-10% around their nominal value for safe operation of the system [1]. The intermittency of solar photovoltaic (PV) generation, together with sudden variations in demand, can induce large voltage fluctuations. At the same time, the power electronic interface from inverter-based resources provides controllability to regulate voltages through the changes of reactive power injections [1]–[5]. A large body of existing research has focused on developing voltage control strategies based on the LinDistflow model, which is a linearized power flow model that characterizes the relation between voltage magnitude and power injections across the distribution network [6]–[10]. This offers tractability and computational efficiency for deriving optimal voltage control policies. However, such linear approximations often fail to capture the nonlinear nature of the power flow model, leading to solutions that can become infeasible or ineffective in practice. This issue becomes increasingly common and pronounced, particularly under light net loading conditions, a scenario that is becoming more prevalent with the growing penetration of distributed energy resources (DERs) [11], [12].

Yiwei Dong and Wenqi Cui are with the Department of Electrical and Computer Engineering, New York University, NY 11201, USA.

Han Xu, Adam Wierman, and Steven Low, are with the Department of Computing + Mathematical Sciences, California Institute of Technology, CA 91125, USA.

The authors are partially supported by the Henry Luce Foundation, the Resnik Sustainability Institute, the PIMCO Foundation.

Optimal power flow-based formulations are proposed to solve voltage control with nonlinear system models [13]–[15]. Several convex relaxations have been developed to transform the resulting nonconvex optimization problems into convex ones, such as second-order cone programs, semidefinite programs [13]–[15]. While the action obtained through convex relaxation is exact when the system is radial and heavily loaded, the optimality gap might be large otherwise [11], [16]. In addition, solving the convex relaxation usually requires the exact information of the topologies and parameters of the distribution system, which may not be available in many distribution systems.

To overcome this challenge, data-driven approaches have been proposed [17]–[19]. Model-free reinforcement learning-based methods are proposed in [20], [21] to learn voltage controllers from data collected during interaction with the system. Performance guarantees are generally built on linearized system models (i.e., LinDistFlow model). To handle the nonlinearity of the power flow models, a convex neural network is adopted in [17] to learn the nonlinear mapping between voltage deviations and power injections. The neural network-based model is subsequently embedded into voltage optimization problem to find optimal power injections. For efficient utilization of online data, [22]–[24] propose feedback optimization approaches to update control actions based on sensitivity estimation of changes in bus voltage magnitudes with respect to changes in reactive power injections. However, these approaches typically rely on gradient descent-based iterations for solution updates, which tend to converge slowly and may struggle to adapt to time-varying loads during real-time operation. In addition, the distance between the converged solution and the original nonlinear optimization problem is generally not guaranteed.

More generally, similar challenges in handling nonlinear dynamics show up in many other control problems [25]–[28], including autonomous driving, space vehicle control, motion planning etc. In particular, [28] proposes to successively convexify the nonlinear control problem by linearizing the dynamics around the iterates of operating points. The convergence to the Karush–Kuhn–Tucker (KKT) point is established. Sequential convex programming is also adopted in [29] to solve optimal power flow based voltage control. However, this approach depends on the exact model information. This paper seeks to address the following question: Can we solve the optimal control problem through successive linearization in a data-driven manner, while still achieving convergence guarantees?

In this paper, we propose a data-driven successive linearization approach to address voltage control with non-

linear power flow models. By leveraging the fact that a nonlinear system is not far away from its linearization when the operating point is close to the linearization point, we perform data-driven linearization around the most recent operating point through using the information of past trajectory measurements. This procedure yields a sequence of data-driven convex surrogates along the trajectory, each of which is solved to optimality at every iteration. Convergence results to a neighborhood of KKT points are established by bounding the discrepancy between the original nonlinear model and its convex surrogate through trust regions. Case study demonstrates that the proposed method achieves faster convergence and adapts quickly to changes in net load.

Contributions of this work are summarized as follows:

- 1) We propose a data-driven successive linearization framework for voltage control with nonlinear power flow models, which leverage the most recent operating trajectories to effectively approximate nonlinear system behavior near the current operating point.
- 2) The proposed framework establishes a formal convergence guarantee to the neighborhood of KKT points of optimal voltage control problem with nonlinear power flow models.
- 3) Case studies show that the proposed method converges rapidly and adapts quickly to changes in net load. It achieves costs comparable to, or lower than, those obtained using model-based convex relaxations.

Notation. Throughout this manuscript, vectors are denoted in lower-case bold, matrices are denoted in upper-case bold, and scalars are unbolded. Subscript (i) indicates variables for the node i . For variables $a_{(1)}, \dots, a_{(n)}$, $\mathbf{a} := (a_{(1)}, \dots, a_{(n)})$ denote the stacked column vector, and \mathbf{a}_k denotes its value at time step k . Unless specified otherwise, $\|\cdot\|$ denotes the Euclidean two-norm.

II. MODEL AND MOTIVATIONS

A. Model

Consider a distribution system with n buses, let $y_{(i)}$ be the voltage at bus i and $\mathbf{y} := (y_{(1)}, \dots, y_{(n)})$ be the voltage across the network. Let $\mathbf{u} := (u_{(1)}, \dots, u_{(n)})$ be the controllable reactive power across the network, and \mathcal{U} , \mathcal{Y} represent the convex and compact feasible set for \mathbf{u} and \mathbf{y} , respectively. Our objective is to control the reactive power injection to reduce voltage deviation from its reference value \mathbf{y}^{ref} , while reducing the incurred control effort. Let $\mathbf{y} = \mathbf{g}(\mathbf{u})$ represents the relation between the reactive power injections and voltage magnitudes, we formulate the voltage control problem as

$$\begin{aligned} \min_{\mathbf{u}, \mathbf{y}} \quad & c_v(\mathbf{y}) + c_u(\mathbf{u}) \\ \text{s.t.} \quad & \mathbf{y} = \mathbf{g}(\mathbf{u}), \quad \mathbf{u} \in \mathcal{U}, \quad \mathbf{y} \in \mathcal{Y} \end{aligned} \quad (1)$$

where $c_v(\cdot)$ and $c_u(\cdot)$ are convex cost function on voltage deviations and control effort, respectively. The costs depends on the type of resources and can be either quadratic [30], [31] or non-quadratic [32]–[34].

The mapping from reactive power injections to voltage magnitudes, $\mathbf{y} = \mathbf{g}(\mathbf{u})$, is defined implicitly by the nonlinear DistFlow equations [35], [36]. In particular, for a given \mathbf{u} , the voltage is obtained by solving the following equations:

$$y_{(i)}^2 = y_{(j)}^2 + 2r_{ij}P_{ij} + 2x_{ij}Q_{ij} - |z_{ij}|^2l_{ij}, \quad (2a)$$

$$\sum_{h: j \rightarrow h} P_{jh} = P_{ij} - r_{ij}l_{ij} + p_{(j)}, \quad (2b)$$

$$\sum_{h: j \rightarrow h} Q_{jh} = Q_{ij} - x_{ij}l_{ij} + u_{(j)}, \quad (2c)$$

$$l_{ij} = (P_{ij}^2 + Q_{ij}^2) / y_{(i)}^2 \quad (2d)$$

where $p_{(j)}$ is the active power injections at node j . For the line connecting nodes i and j , P_{ij} and Q_{ij} denote the active and reactive power flows, r_{ij} and x_{ij} are the line resistance and reactance, and l_{ij} is the squared current magnitude on the line. The complex impedance is $z_{ij} = r_{ij} + jx_{ij}$, and the notation $h: j \rightarrow h$ denotes the set of children of node j . We assume that operating points are not near the voltage-collapse boundary, namely, the Jacobian of the Distflow equation with respect to state variables is nonsingular and not close to singular. This is a common assumption for voltage control, which ensures that the solution of (2) exists [37]. Combined with the Implicit Function Theorem [38], this guarantees that the DistFlow equations induce a locally unique solution mapping $\mathbf{g}: \mathbf{u} \mapsto \mathbf{y}$ that is continuously differentiable. Note that it is generally difficult to explicitly characterize the function $\mathbf{y} = \mathbf{g}(\mathbf{u})$ from (2), and one of the benefits brought by the proposed method is that we do not require the analytical form of \mathbf{g} as prior knowledge.

A series of works has been established in solving (1) (2) through convex relaxation of the DistFlow [14], [39]. For example, converting the line loss function in (2d) to inequality constraints can convert the problem into second-order cone program. The exactness of convex relaxation has also been established [13]. However, these approaches rely on exact model information, which may not be available for many distribution networks.

To eliminate the reliance on exact model information, we consider data-driven methods that update control actions based on system measurements. Existing methods typically use data measurement to approximate the gradient $\nabla_{\mathbf{u}_k} c(\mathbf{u}_k)$ and update control actions iteratively through $\mathbf{u}_{k+1} = \text{Proj}_{\mathcal{U}}(\mathbf{u}_k - \gamma \nabla_{\mathbf{u}_k} c(\mathbf{u}_k))$ with $\text{Proj}_{\mathcal{U}}$ being the projection operator to \mathcal{U} and γ being the learning rate [22], [40]–[42]. For example, feedback optimization computes the gradient by $\nabla_{\mathbf{u}_k} c(\mathbf{u}_k) = \nabla_{\mathbf{u}_k} \mathbf{g}(\mathbf{u}_k) \nabla_{\mathbf{y}_k} c_v(\mathbf{y}_k) + \nabla_{\mathbf{u}_k} c_u(\mathbf{u}_k)$, where the Jacobian matrix $\nabla_{\mathbf{u}_k} \mathbf{g}(\mathbf{u}_k)$ is calculated from the online input-output data [22]. However, gradient-based updates may require a long horizon to converge, and the quality of the converged solution is generally not guaranteed.

B. Successive Linearization

To avoid the slow convergence of gradient descent in data-driven approaches, we propose to leverage the structure of the Problem that the only non-convexity in Problem (1) comes from the nonlinear Distflow in (2). Linearizing the Distflow

will convert (1) to a convex problem, which allows us to solve it to optimality without being restricted to gradient-descent-type updates. Motivated by this, we solve the Problem (1) by successively linearizing the dynamical system at the operating point \mathbf{u}_k for iterations $k = 1, 2, \dots, N$. Specifically, we initialize \mathbf{u}_1 as the current operating point. For each $k = 1, \dots, N-1$, \mathbf{u}_{k+1} is obtained by solving the optimization problem

$$\min_{\mathbf{u}, \mathbf{y}} c_v(\mathbf{y}) + c_u(\mathbf{u}) \quad (3a)$$

$$\text{s.t. } \mathbf{y} = \mathbf{y}_k + \nabla_{\mathbf{u}_k} \mathbf{g}(\mathbf{u}_k) (\mathbf{u} - \mathbf{u}_k), \quad (3b)$$

$$\mathbf{u} \in \mathcal{U}, \quad \mathbf{y} \in \mathcal{Y} \quad (3c)$$

where $\nabla_{\mathbf{u}_k} \mathbf{g}(\mathbf{u}_k)$ is the Jacobian of the function $\mathbf{g}(\mathbf{u})$ at the operating point \mathbf{u}_k .

For trajectories that remain sufficiently close to the operating point \mathbf{u}_k , it is reasonable to regard them as being generated by the local linearization in (3b), which enables the use of trajectory data to construct a data-driven linear approximation of the underlying nonlinear system. However, two fundamental challenges arise. First, data-driven approximations inevitably introduce modeling errors in the resulting linearized dynamics. Second, even when locally accurate, the resulting linearized model may deviate substantially from the original nonlinear DistFlow equations, potentially leading to large optimality gaps when solutions derived from the linear model are applied to the nonlinear problem. These challenges make it nontrivial to ensure convergence of data-driven linearized control schemes.

To address these issues, we develop a data-driven successive linearization framework equipped with a trust region mechanism. This approach enables efficient use of the most recent trajectory data to iteratively refine the local linearized model while ensuring that the induced modeling errors remain bounded. In the following sections, we present the design of the proposed data-driven successive linearization method for the optimal voltage control problem and demonstrate how convergence guarantees are achieved through the trust region mechanism.

III. DATA-DRIVEN SUCCESSIVE LINEARIZATION

In this section, we first introduce the overall framework for data-driven successive linearization with a trust region mechanism. We then present the detailed computational procedures and the corresponding algorithmic design.

A. Successive Linearization with Trust Region Mechanism

To explicitly compute the Jacobian with respect to each operating point $\nabla_{\mathbf{u}_k} \mathbf{g}(\mathbf{u}_k)$, we will need the information of the model $\mathbf{g}(\mathbf{u})$. This would be difficult to be obtained for systems without exact model information or parameters. Therefore, to avoid relying on such model information, we instead resort to a data-driven approach to estimate $\nabla_{\mathbf{u}_k} \mathbf{g}(\mathbf{u}_k)$ through the past trajectory $\{(\mathbf{y}_{k-\tau}, \mathbf{u}_{k-\tau}), \dots, (\mathbf{y}_k, \mathbf{u}_k)\}$.

We consider the estimation of $\nabla_{\mathbf{u}_k} \mathbf{g}(\mathbf{u}_k)$ as finding the sensitivity matrix \mathbf{S}_k that maps perturbations of the input \mathbf{u}

to the changes of output \mathbf{y} :

$$\Delta \mathbf{y}_k \approx \mathbf{S}_k \Delta \mathbf{u}_k,$$

where the details of computing the sensitivity matrix will be given in the next subsection.

Combined with a trust region mechanism to bound the changes of \mathbf{u} , the data-driven approach to solving (1) is thus formulated as

$$\min_{\mathbf{u} \in \mathcal{U}, \mathbf{y} \in \mathcal{Y}} c_v(\mathbf{y}) + c_u(\mathbf{u}) \quad (4a)$$

$$\text{s.t. } \mathbf{y} = \mathbf{y}_k + \tilde{\mathbf{S}}_k (\mathbf{u} - \mathbf{u}_k), \quad (4b)$$

$$\|\mathbf{u} - \mathbf{u}_k\| \leq r_k, \quad (4c)$$

where $\tilde{\mathbf{S}}_k$ is the estimation of the Jacobian $\nabla_{\mathbf{u}_k} \mathbf{g}(\mathbf{u}_k)$, r_k is the radius of the trust region for updating \mathbf{u} at iteration k . The equation (4b) represents the data-driven linearized power flow constraint around the operating point \mathbf{u}_k . The trust region design is motivated by [28] and plays a central role in guaranteeing convergence to the solution of Problem (1) (detailed theorem and proof will be given in Section IV). Iterating this process gives the sequence of solutions $\{(\mathbf{y}_1, \mathbf{u}_1), \dots, (\mathbf{y}_N, \mathbf{u}_N)\}$.

Although the trust region is a hyperparameter to be tuned, its scheme to update control action differs fundamentally from gradient descent-based approaches. In particular, the trust-region subproblem (4) is solved to optimality at every step, enabling it to more effectively exploit the local optimization landscape. Benefiting from this, the proposed approach is less sensitive to parameter tuning and converges faster. In contrast, gradient-based methods usually require a conservative stepsize to avoid oscillations or instability, which can significantly slow convergence. We demonstrate these differences in case studies.

B. Computation of the Sensitivity Matrix

We estimate the Jacobian $\nabla_{\mathbf{u}_k} \mathbf{g}(\mathbf{u}_k)$ by solving a weighted least-squares (WLS) problem [22]:

$$\tilde{\mathbf{S}}_k = \underset{\mathbf{S}}{\operatorname{argmin}} \sum_{l=k-\tau+1}^k \lambda^{k-l} \|\Delta \mathbf{y}_l - \mathbf{S} \Delta \mathbf{u}_l\|^2, \quad (5)$$

where $\Delta \mathbf{u}_l := \mathbf{u}_l - \mathbf{u}_{l-1}$ and $\Delta \mathbf{y}_l := \mathbf{y}_l - \mathbf{y}_{l-1}$ denote the first-order differences of the reactive-power injections and bus voltages, respectively. The parameter τ is the length of the window used for sensitivity estimation, and $\lambda \in (0, 1)$ is the forgetting factor that assigns less weight to older measurements.

To express the WLS solution to (5) in matrix form, we stack $\Delta \mathbf{u}_l$ and $\Delta \mathbf{y}_l$ as rows and define

$$\mathbf{U} := \begin{bmatrix} \Delta \mathbf{u}_{k-\tau+1}^\top \\ \vdots \\ \Delta \mathbf{u}_k^\top \end{bmatrix} \in \mathbb{R}^{\tau \times n}, \quad \mathbf{Y} := \begin{bmatrix} \Delta \mathbf{y}_{k-\tau+1}^\top \\ \vdots \\ \Delta \mathbf{y}_k^\top \end{bmatrix} \in \mathbb{R}^{\tau \times n}. \quad (6)$$

The forgetting-factor weights can then be collected into a diagonal matrix $\mathbf{W} \in \mathbb{R}^{\tau \times \tau}$ with

$$\mathbf{W} := \operatorname{diag}(\lambda^{\tau-1}, \lambda^{\tau-2}, \dots, \lambda, 1), \quad (7)$$

so that the cost in (5) can be written as

$$\ell(\mathbf{S}) = \|\mathbf{W}^{1/2}(\mathbf{Y} - \mathbf{U}\mathbf{S}^\top)\|_F^2, \quad (8)$$

where $\|\cdot\|_F$ denotes the Frobenius norm.

The length τ of the past trajectory for computing the sensitivity estimation is determined based on sufficient excitation condition of matrix \mathbf{U} defined as follows:

Definition 1 (Sufficient excitation). *The past trajectory $\{\Delta\mathbf{u}_l, \Delta\mathbf{y}_l\}$ for $l = k - \tau + 1, \dots, k$ is said to be sufficiently excited if the matrix \mathbf{U} in (6) is full column rank.*

When the sufficient excitation condition holds, the WLS estimator admits the closed-form solution

$$\tilde{\mathbf{S}}_k^\top = (\mathbf{U}^\top \mathbf{W} \mathbf{U})^{-1} \mathbf{U}^\top \mathbf{W} \mathbf{Y}. \quad (9)$$

Ideally, perturbations of \mathbf{u} should be conducted around the operating point of interest. This would require the system to be ‘fixed’ around the point and add small perturbations until the sufficient excitation of \mathbf{U} is satisfied. However, such a procedure would substantially increase the amount of data required and slow convergence. Therefore, we hope that the system can perform optimization at each action step, instead of ‘fixed’ and perturb around the current operating point. Notably, we find that the difference between the estimated sensitivity and the true Jacobian can be bounded by the trust region r_k . Properly setting the trust region allows us to use the past trajectory efficiently and still achieve convergence guarantees. Details will follow in Section IV.

C. Algorithm

The data-driven successive linearization method for solving (1) proceeds as follows. At iteration k , we estimate the local Jacobian matrix via weighted least squares (5) using recent input–output increments. This gives us the data-driven linearized model $\mathbf{y} = \mathbf{y}_k + \tilde{\mathbf{S}}_k(\mathbf{u} - \mathbf{u}_k)$. Solving the trust-region subproblem (4) to optimality then produces the next iterate \mathbf{u}_{k+1} . After applying \mathbf{u}_{k+1} and measuring \mathbf{y}_{k+1} , we refresh the data collection buffer and repeat the above process. The complete procedure of the data-driven successive linearization method is summarized in Algorithm 1.

IV. CONVERGENCE ANALYSIS

This section establishes convergence of the data-driven successive linearization method. We first introduce notations and assumptions, and then present the main theorem and proofs for the data-driven successive linearization.

A. Main Theorem

For notational convenience in the convergence analysis, let $\mathbf{z} := (\mathbf{y}, \mathbf{u})$ and define the constraint residual $\mathbf{e}(\mathbf{z}) := \mathbf{y} - \mathbf{g}(\mathbf{u})$. In this way, the equations in Problem 1 are converted to the equality constraints $\mathbf{e}(\mathbf{z}) = \mathbf{0}$, with $\mathbf{e}(\cdot)$ nonconvex and continuously differentiable. Furthermore, we denote $\{\mathbf{z} : \mathbf{h}(\mathbf{z}) \leq 0\}$ as the compact constraint set for \mathbf{z} , where each h_j is convex and continuously differentiable. The requirement for cost functions is specified in the following assumption.

Algorithm 1 Data-driven Successive Linearization

- 1: **Input:** Constraint sets \mathcal{U}, \mathcal{Y} ; costs $c_v(\cdot), c_u(\cdot)$; previous data window of length τ ; forgetting factor $\lambda \in (0, 1)$; initial $(\mathbf{u}_1, \mathbf{y}_1)$; trust-region radius r
- 2: **for** $k = 1, 2, \dots, N - 1$ **do**
- 3: collect $\{\Delta\mathbf{u}_\ell, \Delta\mathbf{y}_\ell\}_{\ell=k-\tau}^k$ with $\Delta\mathbf{u}_\ell = \mathbf{u}_\ell - \mathbf{u}_{\ell-1}$ and $\Delta\mathbf{y}_\ell = \mathbf{y}_\ell - \mathbf{y}_{\ell-1}$
- 4: solve

$$\tilde{\mathbf{S}}_k = \arg \min_{\mathbf{S}} \sum_{\ell=k-\tau+1}^k \lambda^{k-\ell} \|\Delta\mathbf{y}_\ell - \mathbf{S} \Delta\mathbf{u}_\ell\|^2$$

where $(\Delta\mathbf{u}_\ell, \Delta\mathbf{y}_\ell)$ are measured increments

- 5: compute \mathbf{u}_{k+1} by solving the linearized convex trust-region subproblem

$$\begin{aligned} & \min_{\mathbf{u} \in \mathcal{U}, \mathbf{y} \in \mathcal{Y}} c_v(\mathbf{y}) + c_u(\mathbf{u}) \\ & \text{s.t. } \mathbf{y} = \mathbf{y}_k + \tilde{\mathbf{S}}_k(\mathbf{u} - \mathbf{u}_k), \quad \|\mathbf{u} - \mathbf{u}_k\| \leq r \end{aligned}$$

- 6: implement \mathbf{u}_{k+1} and measure \mathbf{y}_{k+1}
 - 7: **end for**
 - 8: **Output:** sequences $\{\mathbf{u}_k\}_{k=1}^N$ and $\{\mathbf{y}_k\}_{k=1}^N$
-

Assumption 1 (Cost regularity). *The cost functions c_v and c_u are convex and continuously differentiable. The composite objective with respect to \mathbf{z} , $c(\mathbf{z}) := c_v(\mathbf{y}) + c_u(\mathbf{u})$, is also convex and continuously differentiable.*

We additionally assume that the Linear Independence Constraint Qualification (LICQ) holds, which is a standard regularity condition in nonlinear optimization and is commonly imposed to establish convergence and stationarity results for nonconvex constrained problems [28], [43], [44].

Assumption 2 (LICQ). *Let \mathcal{J}_{eq} index the equality constraints in $\mathbf{e}(\mathbf{z}) = \mathbf{0}$ and $\mathcal{J}_{\text{ineq}}$ index the inequalities $\{h_j(\mathbf{z}) \leq 0\}$. Define the active set $\mathcal{J}_{\text{ac}}(\mathbf{z}) := \{j \in \mathcal{J}_{\text{ineq}} : h_j(\mathbf{z}) = 0\}$. LICQ holds at \mathbf{z} if the set of gradients*

$$\{\nabla e_i(\mathbf{z}) : i \in \mathcal{J}_{\text{eq}}\} \cup \{\nabla h_j(\mathbf{z}) : j \in \mathcal{J}_{\text{ac}}(\mathbf{z})\}$$

is linearly independent.

Under LICQ in Assumption (2), the KKT conditions provide first-order necessary conditions for local optimality.

Definition 2 (KKT conditions for (1)). *A feasible point $\bar{\mathbf{z}}$ is a KKT point of (1) if there exist multipliers $\{\nu_i\}_{i \in \mathcal{J}_{\text{eq}}}$ and $\{\mu_j\}_{j \in \mathcal{J}_{\text{ac}}(\bar{\mathbf{z}})}$ with $\mu_j \geq 0$ such that*

$$\nabla c(\bar{\mathbf{z}}) + \sum_{i \in \mathcal{J}_{\text{eq}}} \nu_i \nabla e_i(\bar{\mathbf{z}}) + \sum_{j \in \mathcal{J}_{\text{ac}}(\bar{\mathbf{z}})} \mu_j \nabla h_j(\bar{\mathbf{z}}) = \mathbf{0}.$$

Definition 2 characterizes first-order optimality for the original constrained Problem 1. For the convergence analysis of the data-driven successive linearization, it is convenient to work with an exact-penalty reformulation that aggregates the constraints into the objective, and then find the corresponding optimality conditions. We therefore introduce the penalty problem and the associated stationary set.

For the exact penalty objective, we minimize the cost:

$$J(\mathbf{z}) := c(\mathbf{z}) + \boldsymbol{\lambda}^\top |\mathbf{e}(\mathbf{z})| + \boldsymbol{\eta}^\top [\mathbf{h}(\mathbf{z})]_+, \quad (10)$$

with penalty vectors $\boldsymbol{\lambda} \geq \mathbf{0}$, $\boldsymbol{\eta} \geq \mathbf{0}$, and $[\mathbf{h}(\mathbf{z})]_+ := \max\{\mathbf{h}(\mathbf{z}), \mathbf{0}\}$ is applied componentwise. The stationary set for $\min_{\mathbf{z}} J(\mathbf{z})$ is $\mathcal{T} := \{\mathbf{z} : \mathbf{0} \in \partial J(\mathbf{z})\}$, where ∂J denotes the generalized differential. By Theorem 3.9 of [28], for sufficiently large penalties, any stationary point $\bar{\mathbf{z}} \in \mathcal{T}$ that is feasible for (1) is a KKT point of the original problem. Thus it suffices to show that the data-driven successive linearization iterates approach \mathcal{T} for (10). We have the following theorem.

Theorem 1. *Let Assumptions 1–2 hold. Then the data-driven successive linearization algorithm always has limit points. If the Jacobian estimation error vanishes, then any limit point $\bar{\mathbf{z}}$ is a stationary point of (10). Furthermore, if $\bar{\mathbf{z}}$ is feasible for the original problem (1), then $\bar{\mathbf{z}}$ is a KKT point of (1).*

We establish the theorem as follows. First, we show that the distance between the data-driven linearized penalty objective and the accurate penalty objective can be bounded by trust region. This further yields a uniform estimate linking the decrease of the data-driven linearized objective to the true decrease of the original problem in a neighborhood of any nonstationary point at each step. Combining this relation with optimality conditions of the linearized penalty subproblem, we show that the algorithm admits limit points that lie within a neighborhood of stationary points. When the limit point is stationary for the penalized problem and also satisfies the original constraints, exact-penalty theory [28] together with the LICQ assumption implies that it satisfies the KKT conditions of the original problem. The next subsection presents a detailed proof following this outline.

B. Proof of Theorem 1

To relate the cost arising from successive linearization to the cost under the nonlinear model $J(\mathbf{z})$, we introduce the following penalized cost functions. For iteration step k , we have the decision variables $\mathbf{z}_k = (\mathbf{y}_k, \mathbf{u}_k)$, and recall that the original problem enforces the equality constraint $\mathbf{e}(\mathbf{z}_k) = \mathbf{y}_k - \mathbf{g}(\mathbf{u}_k) = \mathbf{0}$. For notational convenience, we denote $\mathbf{S}_k := \nabla_{\mathbf{u}_k} \mathbf{g}(\mathbf{u}_k)$ throughout the remainder of the paper. Define the step

$$\mathbf{d} := (\mathbf{d}_y, \mathbf{d}_u) := (\mathbf{y} - \mathbf{y}_k, \mathbf{u} - \mathbf{u}_k). \quad (11)$$

The penalized cost associated with the model linearized at \mathbf{z}_k is

$$\begin{aligned} L_k(\mathbf{d}) &:= c_v(\mathbf{y}_k + \mathbf{d}_y - \mathbf{y}^{\text{ref}}) + c_u(\mathbf{u}_k + \mathbf{d}_u) \\ &+ \boldsymbol{\lambda}^\top |\mathbf{d}_y - \mathbf{S}_k \mathbf{d}_u| + \boldsymbol{\eta}^\top [\mathbf{h}(\mathbf{y}_k + \mathbf{d}_y, \mathbf{u}_k + \mathbf{d}_u)]_+. \end{aligned} \quad (12)$$

The data-driven counterpart replaces \mathbf{S}_k by the data-driven estimate $\tilde{\mathbf{S}}_k$:

$$\begin{aligned} \tilde{L}_k(\mathbf{d}) &:= c_v(\mathbf{y}_k + \mathbf{d}_y - \mathbf{y}^{\text{ref}}) + c_u(\mathbf{u}_k + \mathbf{d}_u) \\ &+ \boldsymbol{\lambda}^\top |\mathbf{d}_y - \tilde{\mathbf{S}}_k \mathbf{d}_u| + \boldsymbol{\eta}^\top [\mathbf{h}(\mathbf{y}_k + \mathbf{d}_y, \mathbf{u}_k + \mathbf{d}_u)]_+. \end{aligned} \quad (13)$$

Note that $L_k(\mathbf{0}) = \tilde{L}_k(\mathbf{0}) = J(\mathbf{z}_k)$. The map $\mathbf{d} \mapsto \mathbf{d}_y - \tilde{\mathbf{S}}_k \mathbf{d}_u$ is affine, and \mathbf{h} is convex; since compositions with $|\cdot|$ and $[\cdot]_+$ preserve convexity, \tilde{L}_k is a convex surrogate of J in a neighborhood of \mathbf{z}_k . For the convergence proof, we need the solution \mathbf{d}_k^* of the following convex trust-region subproblem at each iteration k :

$$\begin{aligned} \min_{\mathbf{d}} \quad & \tilde{L}_k(\mathbf{d}) \\ \text{s.t.} \quad & \|\mathbf{d}\| \leq r_k, \end{aligned} \quad (14)$$

with the trust-region radius $r_k > 0$.

To analyze the convergence of the data-driven successive linearization method, we need to control the error incurred by replacing the true sensitivity with its data-driven estimate over the trust region. The next lemma provides a bound on this discrepancy.

Lemma 1. *Suppose the sensitivity estimation window $\{k - \tau + 1, \dots, k\}$ satisfies $\max_{\ell \in \{k - \tau + 1, \dots, k\}} \|\mathbf{z}_\ell - \mathbf{z}_k\| \leq \alpha r_k$ for some $\alpha > 0$. Then, for every \mathbf{z} with $\|\mathbf{z} - \mathbf{z}_k\| \leq r_k$, letting $\tilde{\mathbf{S}}_k$ be the weighted least-squares estimate for (5), we have*

$$\|(\tilde{\mathbf{S}}_k - \mathbf{S}_k)(\mathbf{u} - \mathbf{u}_k)\| = o(r_k) \text{ as } r_k \rightarrow 0. \quad (15)$$

We prove the lemma by exploiting a closed-form representation of the estimated sensitivity matrix $\tilde{\mathbf{S}}_k$ constructed from the past trajectories of the control inputs \mathbf{u} and voltage states \mathbf{y} . This enables a precise comparison between $\tilde{\mathbf{S}}_k$ and the Jacobian \mathbf{S}_k by leveraging local Lipschitz continuity and the trust-region bound on recent iterates. The detailed proof is given in Appendix A.

Lemma 1 implies that the norm of $(\tilde{\mathbf{S}}_k - \mathbf{S}_k)(\mathbf{u} - \mathbf{u}_k)$ is $o(r_k)$ uniformly for all \mathbf{z} with $\|\mathbf{z} - \mathbf{z}_k\| \leq r_k$. The next two lemmas compare the nonlinear penalized objective with its linearized surrogates in this trust region.

Lemma 2. *For every \mathbf{d} with $\|\mathbf{d}\| \leq r_k$,*

$$J(\mathbf{z}_k + \mathbf{d}) = L_k(\mathbf{d}) + o(r_k). \quad (16)$$

Proof. The functions c_v , c_u , and the convex-inequality penalty $\boldsymbol{\eta}^\top [\mathbf{h}(\mathbf{y}_k + \mathbf{d}_y, \mathbf{u}_k + \mathbf{d}_u)]_+$ appear identically in both $J(\mathbf{z}_k + \mathbf{d})$ and $L_k(\mathbf{d})$ and hence cancel in their difference. By a second-order Taylor expansion of \mathbf{g} at \mathbf{u}_k , for any step \mathbf{d}_u we can write $\mathbf{g}(\mathbf{u}_k + \mathbf{d}_u) = \mathbf{g}(\mathbf{u}_k) + \mathbf{S}_k \mathbf{d}_u + \boldsymbol{\gamma}_k(\mathbf{d}_u)$, where the higher-order residual satisfies $\|\boldsymbol{\gamma}_k(\mathbf{d}_u)\| \leq \beta \|\mathbf{d}_u\|^2$ for all \mathbf{d}_u with some constant $\beta > 0$. By the triangle inequality,

$$\begin{aligned} & J(\mathbf{z}_k + \mathbf{d}) - L_k(\mathbf{d}) \\ &= \boldsymbol{\lambda}^\top (|\mathbf{d}_y - \mathbf{S}_k \mathbf{d}_u - \boldsymbol{\gamma}_k(\mathbf{d}_u)| - |\mathbf{d}_y - \mathbf{S}_k \mathbf{d}_u|) \\ &\leq \|\boldsymbol{\lambda}\| \|\boldsymbol{\gamma}_k(\mathbf{d}_u)\| \leq c \|\boldsymbol{\lambda}\| \|\mathbf{d}_u\|^2 \leq c \|\boldsymbol{\lambda}\| \|\mathbf{d}\|^2, \end{aligned} \quad (17)$$

which yields (16). \square

Lemma 3. *Suppose the assumptions in Lemma 1 hold. Then the difference between the data-driven surrogate \tilde{L}_k and the exact linearized model L_k satisfies*

$$|\tilde{L}_k(\mathbf{d}) - L_k(\mathbf{d})| = o(r_k) \text{ for all } \|\mathbf{d}\| \leq r_k. \quad (18)$$

In addition, the following relation holds for J and \tilde{L}_k :

$$J(\mathbf{z}_k + \mathbf{d}) = \tilde{L}_k(\mathbf{d}) + o(r_k) \text{ for all } \|\mathbf{d}\| \leq r_k. \quad (19)$$

Proof. By the definition of L_k and \tilde{L}_k ,

$$\tilde{L}_k(\mathbf{d}) - L_k(\mathbf{d}) = \boldsymbol{\lambda}^\top \left(|\mathbf{d}_y - \tilde{\mathbf{S}}_k \mathbf{d}_u| - |\mathbf{d}_y - \mathbf{S}_k \mathbf{d}_u| \right).$$

Using the triangle inequality componentwise and then Cauchy-Schwarz inequality,

$$\begin{aligned} |\tilde{L}_k(\mathbf{d}) - L_k(\mathbf{d})| &\leq \boldsymbol{\lambda}^\top |(\tilde{\mathbf{S}}_k - \mathbf{S}_k) \mathbf{d}_u| \\ &\leq \|\boldsymbol{\lambda}\| \|(\tilde{\mathbf{S}}_k - \mathbf{S}_k) \mathbf{d}_u\|. \end{aligned} \quad (20)$$

Since $\|\mathbf{d}\| \leq r_k$ and $\mathbf{d}_u = \mathbf{u} - \mathbf{u}_k$, Lemma 1 yields $\|(\tilde{\mathbf{S}}_k - \mathbf{S}_k) \mathbf{d}_u\| = o(r_k)$, and hence (18) follows from (20). For (19), write

$$\begin{aligned} J(\mathbf{z}_k + \mathbf{d}) &= L_k(\mathbf{d}) + (J(\mathbf{z}_k + \mathbf{d}) - L_k(\mathbf{d})) \\ &= \tilde{L}_k(\mathbf{d}) + (L_k(\mathbf{d}) - \tilde{L}_k(\mathbf{d})) + (J(\mathbf{z}_k + \mathbf{d}) - L_k(\mathbf{d})). \end{aligned} \quad (21)$$

By (18) and Lemma 2, the equality in (19) holds. \square

The above lemma shows that the penalized objective admits a local approximation by the data-driven linearized model. Since the proposed data-driven successive linearization solves the convex trust-region subproblem to optimality, we can relate the cost decrease achieved on the nonlinear penalized objective to the decrease suggested by the linearized model within the same step. For any point \mathbf{z} and step \mathbf{d} , define the decreases in the nonlinear penalized objective and its data-driven linearized counterpart as

$$\begin{aligned} \Delta J(\mathbf{z}, \mathbf{d}) &:= J(\mathbf{z}) - J(\mathbf{z} + \mathbf{d}), \\ \Delta \tilde{L}(\mathbf{z}, \mathbf{d}) &:= J(\mathbf{z}) - \tilde{L}(\mathbf{d}). \end{aligned} \quad (22)$$

The ratio

$$\rho(\mathbf{z}, r) := \frac{\Delta J(\mathbf{z}, \mathbf{d})}{\Delta \tilde{L}(\mathbf{z}, \mathbf{d})} \quad (23)$$

quantifies the agreement between the decrease of the nonlinear penalized objective and the decrease measured by the data-driven linearized model along the step \mathbf{d} . The next lemmas relate $\Delta J(\mathbf{z}, \mathbf{d})$ and $\Delta \tilde{L}(\mathbf{z}, \mathbf{d})$ obtained from the data-driven linearized trust-region subproblem.

Lemma 4. *For any iteration k and radius $r_k > 0$, let \mathbf{d}_k^* be a minimizer of the trust-region subproblem (14) with $\|\mathbf{d}_k^*\| \leq r_k$. Then*

$$\Delta \tilde{L}_k(\mathbf{z}_k, \mathbf{d}_k^*) = J(\mathbf{z}_k) - \tilde{L}_k(\mathbf{d}_k^*) \geq 0. \quad (24)$$

If equality holds in (24), then $\mathbf{0} \in \partial \tilde{L}_k(\mathbf{0})$ and

$$\text{dist}(\mathbf{0}, \partial J(\mathbf{z}_k)) \leq \|\boldsymbol{\lambda}\| \|\tilde{\mathbf{S}}_k - \mathbf{S}_k\|. \quad (25)$$

In particular, if $\tilde{\mathbf{S}}_k = \mathbf{S}_k$, then $\mathbf{0} \in \partial J(\mathbf{z}_k)$, i.e., $\mathbf{z}_k \in \mathcal{T}$.

Proof. First, the zero step $\mathbf{d} = \mathbf{0}$ is feasible for (14). By construction of the linearized model at \mathbf{z}_k , $\tilde{L}_k(\mathbf{0}) = J(\mathbf{z}_k)$. Since \mathbf{d}_k^* minimizes \tilde{L}_k over $\{\mathbf{d} : \|\mathbf{d}\| \leq r_k\}$,

$$\tilde{L}_k(\mathbf{d}_k^*) \leq \tilde{L}_k(\mathbf{0}) = J(\mathbf{z}_k),$$

and (24) follows.

Assume now that equality holds in (24). Then $\tilde{L}_k(\mathbf{d}_k^*) = \tilde{L}_k(\mathbf{0})$, so $\mathbf{0}$ is also a minimizer of the convex subproblem.

Since $\mathbf{0}$ lies in the interior of the trust region, the first-order optimality condition gives $\mathbf{0} \in \partial \tilde{L}_k(\mathbf{0})$.

To relate $\partial \tilde{L}_k(\mathbf{0})$ and $\partial J(\mathbf{z}_k)$, write $\tilde{L}_k(\mathbf{d}) = \ell_k(\mathbf{d}) + \phi_{\tilde{\mathbf{S}}_k}(\mathbf{d})$, $L_k(\mathbf{d}) = \ell_k(\mathbf{d}) + \phi_{\mathbf{S}_k}(\mathbf{d})$, where $\ell_k(\mathbf{d}) := c(\mathbf{z}_k + \mathbf{d}) + \boldsymbol{\eta}^\top [h(\mathbf{z}_k + \mathbf{d})]_+$ and $\phi_{\mathbf{M}}(\mathbf{d}) := \boldsymbol{\lambda}^\top |\mathbf{d}_y - \mathbf{M} \mathbf{d}_u|$ for any matrix \mathbf{M} . Let $\Xi := \{\boldsymbol{\xi} \in \mathbb{R}^n : |\xi_i| \leq \lambda_i, i = 1, \dots, n\}$. Then, a direct characterization of the generalized differential at $\mathbf{d} = \mathbf{0}$ yields

$$\partial \phi_{\mathbf{M}}(\mathbf{0}) = \left\{ \left[\begin{array}{c} \boldsymbol{\xi} \\ -\mathbf{M}^\top \boldsymbol{\xi} \end{array} \right] : \boldsymbol{\xi} \in \Xi \right\}.$$

Since ℓ_k is identical in L_k and \tilde{L}_k , we have $\partial \tilde{L}_k(\mathbf{0}) = \partial \ell_k(\mathbf{0}) + \partial \phi_{\tilde{\mathbf{S}}_k}(\mathbf{0})$, $\partial L_k(\mathbf{0}) = \partial \ell_k(\mathbf{0}) + \partial \phi_{\mathbf{S}_k}(\mathbf{0})$. Because $\mathbf{0} \in \partial \tilde{L}_k(\mathbf{0})$, there exist $\mathbf{s} \in \partial \ell_k(\mathbf{0})$ and $\boldsymbol{\xi} \in \Xi$ such that

$$\mathbf{s} + \left[\begin{array}{c} \boldsymbol{\xi} \\ -\tilde{\mathbf{S}}_k^\top \boldsymbol{\xi} \end{array} \right] = \mathbf{0}.$$

As the generalized subdifferential induced by exact Jacobian \mathbf{S}_k is

$$\partial L_k(\mathbf{0}) = \left\{ \mathbf{s} + \left[\begin{array}{c} \boldsymbol{\xi} \\ -\mathbf{S}_k^\top \boldsymbol{\xi} \end{array} \right] : \boldsymbol{\xi} \in \Xi \right\},$$

we obtain one vector $\mathbf{v} \in \partial L_k(\mathbf{0})$:

$$\mathbf{v} = \mathbf{s} + \left[\begin{array}{c} \boldsymbol{\xi} \\ -\mathbf{S}_k^\top \boldsymbol{\xi} \end{array} \right] = \left[\begin{array}{c} \mathbf{0} \\ (\tilde{\mathbf{S}}_k - \mathbf{S}_k)^\top \boldsymbol{\xi} \end{array} \right],$$

then $\|\mathbf{v}\| \leq \|\tilde{\mathbf{S}}_k - \mathbf{S}_k\| \|\boldsymbol{\xi}\|$.

Finally, since $e(\mathbf{z}) = \mathbf{y} - \mathbf{g}(\mathbf{u})$ is continuously differentiable at \mathbf{z}_k with Jacobian $[\mathbf{I}, -\mathbf{S}_k]$, the Clarke chain rule implies that the generalized differential of the equality penalty term in J at \mathbf{z}_k coincides with that of $\phi_{\mathbf{S}_k}$ at $\mathbf{d} = \mathbf{0}$; combined with the identical ℓ_k part, this yields $\partial L_k(\mathbf{0}) = \partial J(\mathbf{z}_k)$. Therefore, $\text{dist}(\mathbf{0}, \partial J(\mathbf{z}_k)) = \text{dist}(\mathbf{0}, \partial L_k(\mathbf{0})) \leq \|\mathbf{v}\| \leq \|\boldsymbol{\lambda}\| \|\tilde{\mathbf{S}}_k - \mathbf{S}_k\|$, which proves (25). The special case $\tilde{\mathbf{S}}_k = \mathbf{S}_k$ gives $\mathbf{0} \in \partial J(\mathbf{z}_k)$. \square

Lemma 4 shows that the decrease measured by the data-driven linearized model produced by (14) is always nonnegative. If the algorithm terminates in finitely many iterations because $\Delta \tilde{L}_k(\mathbf{z}_k, \mathbf{d}_k^*) = 0$, then (25) implies that the termination point lies in an $O(\|\tilde{\mathbf{S}}_k - \mathbf{S}_k\|)$ -neighborhood of \mathcal{T} . In the case where $\tilde{\mathbf{S}}_k = \mathbf{S}_k$, this residual vanishes and $\mathbf{z}_k \in \mathcal{T}$; with feasibility for (1), Theorem 3.9 of [28] implies that \mathbf{z}_k is a KKT point of the original problem.

When the proposed algorithm generates an infinite sequence $\{\mathbf{z}_k\}$, the next lemma establishes a lower bound on the ratio $\rho(\mathbf{z}_k, r_k)$ for nonstationary points, which will be used to depict the stationarity of every limit point of $\{\mathbf{z}_k\}$.

Lemma 5. *Let $\bar{\mathbf{z}}$ be feasible for (10) and not stationary. Then there exist $\bar{\epsilon} > 0$, $\bar{r} > 0$, and $\kappa > 0$ such that for any $\mathbf{z}_k \in N(\bar{\mathbf{z}}, \bar{\epsilon})$ and any $r_k \in (0, \bar{r}]$, if \mathbf{d}_k^* minimizes $\tilde{L}_k(\mathbf{d})$ over $\{\mathbf{d} : \|\mathbf{d}\| \leq r_k\}$, then*

$$\rho(\mathbf{z}_k, r_k) := \frac{\Delta J_k(\mathbf{z}_k, \mathbf{d}_k^*)}{\Delta \tilde{L}_k(\mathbf{z}_k, \mathbf{d}_k^*)} \geq 1 - \frac{o(r_k)}{(\kappa/2)r_k + o(r_k)}.$$

The detailed proof of this lemma generally follows arguments in Lemma 3.11 of [28] and is provided in Appendix B

for completeness. Lemma 5 implies that, for sufficiently small trust-region, solving the convex linearized subproblem (14) yields steps whose performance closely reflects the behavior of the original objective, thereby justifying the use of data-driven successive linearization. This result underpins the proof of the next lemma, which establishes convergence to a neighborhood of the stationary point when the proposed algorithm generates an infinite sequence $\{z_k\}$.

Lemma 6. *Let the Assumption 1–2 hold, then the data-driven successive linearization algorithm always has limit points. Let \bar{z} be any limit point, then \bar{z} satisfies the stationarity bound for the penalty problem (10):*

$$\text{dist}(\mathbf{0}, \partial J(\bar{z})) \leq \|\lambda\| \liminf_{i \rightarrow \infty} \|\tilde{\mathbf{S}}_{k_i} - \mathbf{S}_{k_i}\|.$$

The proof is established by contradiction, by showing that any limit point cannot lie outside the corresponding neighborhood of the stationary set of the penalized problem. The detailed proof is given in Appendix C.

The above results establish convergence to a neighborhood of the KKT point. In particular, when the Jacobian estimation error vanishes, \bar{z} is a stationary point of (10), i.e., $\|\tilde{\mathbf{S}}_{k_i} - \mathbf{S}_{k_i}\| \rightarrow 0$ implies $\bar{z} \in \mathcal{T}$. If \bar{z} is feasible for the original problem (1), it means the iterates converge to an exact KKT point of (1). This concludes the proof for Theorem 1. In addition, to make $\|\tilde{\mathbf{S}}_{k_i} - \mathbf{S}_{k_i}\|$ sufficiently close to zero, whenever the algorithm stalls (e.g., the update $\|z_{k+1} - z_k\|$ falls below a prescribed tolerance), one could choose to inject small zero-mean Gaussian perturbations into the control input and then recompute $\tilde{\mathbf{S}}_k$.

V. CASE STUDY

To validate the performance of the proposed data-driven successive linearization method for voltage control, we conduct experiments on the IEEE 33-bus system [45] with both time-invariant and time-varying net load. All electrical quantities are expressed in per unit (p.u.) on a 100 MVA, 12.66 kV base. Each bus has controllable reactive power within ± 0.05 p.u., with a voltage reference of 1.00 p.u. At each step we solve the DistFlow [36] to obtain voltage magnitudes resulting from the current active and reactive power injections. The cost value c_t at each time t is the quadratic voltage-tracking error plus a penalty on the control effort: $c_t = 0.5\|\mathbf{y}_t - \mathbf{1}\|^2 + 0.1\|\mathbf{u}_t\|^2$, where $\mathbf{1}$ denotes the all-one vector. We compare the proposed data-driven successive linearization with the following voltage control methods:

- **Convex Relaxation [13].** Optimal power flow-based voltage control, which solves formulation in (1) using the DistFlow model. Quadratic equality constraints corresponding to line losses are relaxed to be convex inequalities, resulting in a second-order cone program. Details can be found in [13].
- **Feedback Optimization [22].** Update the control input via projected gradient descent $\mathbf{u}_{k+1} = \text{Proj}_{\mathcal{U}}(\mathbf{u}_k - \gamma \nabla_{\mathbf{u}_k} c(\mathbf{u}_k))$ with γ being the learning rate [22]. The gradient of the cost function is computed through

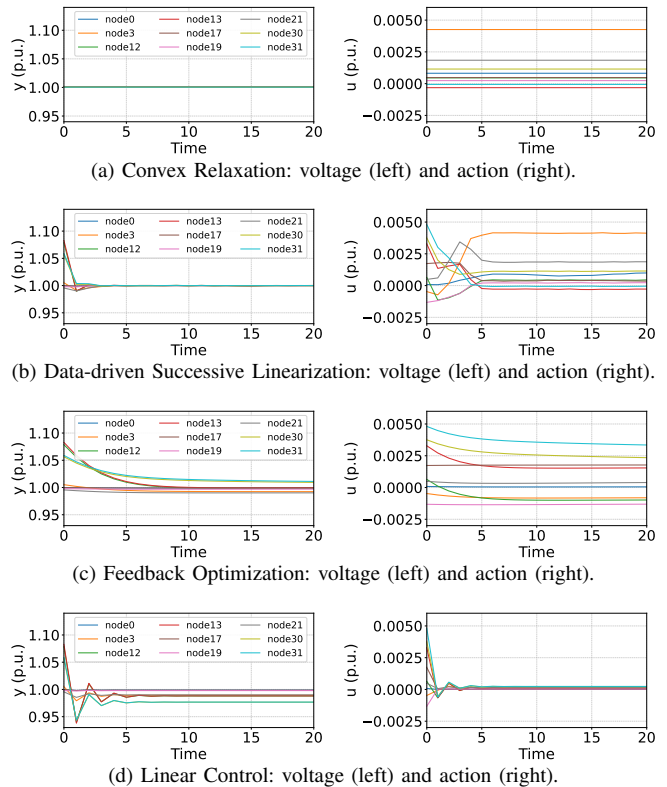


Fig. 1. The voltage and reactive power at 9 nodes under four controllers in the time-invariant load setting. Convex relaxation obtains a solution that is feasible for the original nonconvex problem (1), indicating that it is globally optimal for the original problem. Data-driven successive linearization converges within a few iterations to a solution that is very close to this global optimum. Both feedback optimization and linear control converge more slowly, which also retains larger steady-state voltage deviation.

chain rule as $\nabla_{\mathbf{u}_k} c(\mathbf{u}_k) = \nabla_{\mathbf{u}_k} \mathbf{g}(\mathbf{u}_k) \nabla_{\mathbf{y}_k} c_v(\mathbf{y}_k) + \nabla_{\mathbf{u}_k} c_u(\mathbf{u}_k)$, where the Jacobian matrix $\nabla_{\mathbf{u}_k} \mathbf{g}(\mathbf{u}_k)$ is calculated from the online input-output data through (5).

- **Linear Controller [46].** Linear control law following the IEEE 1547-2018 standard, expressed as $u_{(i)} = \varphi_i(y_{(i)} - 1)$ with φ_i being the linear control gain optimized through learning-based framework in [47].

In the above methods, the convex relaxation requires exact parameters of the DistFlow model, whereas the others are model-free. We first conduct experiments on a system with time-invariant loads to demonstrate the convergence of the proposed method and the optimality of the cost at convergence. Subsequently, we perform experiments with time-varying loads and step changes to illustrate that the proposed method enables fast adaptation to changes in the net load.

A. Time-Invariant Load

Under a fixed load, Fig. 1 demonstrates the voltage and reactive power for 9 selected nodes under different methods. The solution of convex relaxation is shown in Fig. 1(a), which recovers voltages close to 1 p.u. It is noteworthy that this solution is feasible for the original nonconvex voltage control problem, indicating that this solution is the global optimum of the original nonconvex problem (1). The proposed data-driven successive linearization in Fig. 1(b)

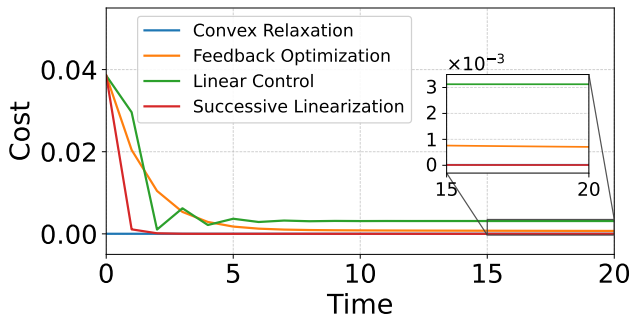


Fig. 2. Cost trajectories corresponding to Fig. 1. Convex relaxation provides a global benchmark. Feedback optimization and linear control retain high costs after convergence. The proposed data-driven successive linearization rapidly drives the cost to the convex relaxation level within a few iterations, indicating fast convergence.

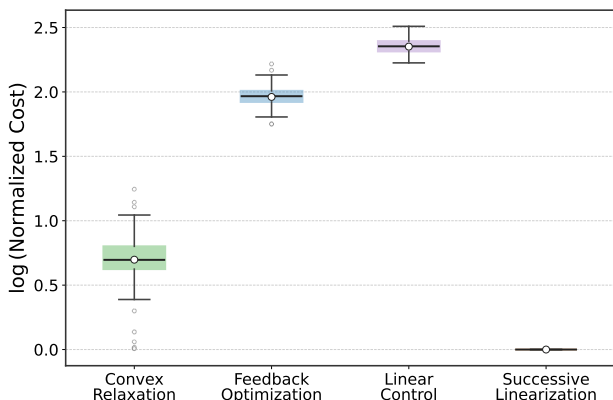


Fig. 3. Comparison of log-normalized mean cost of the last 5 steps in the time-invariant load setting over 100 trials. Data-driven successive linearization consistently achieves the lowest cost, with values tightly concentrated near zero, indicating both superior performance and small deviation across trials.

converges after 3 steps, where the voltage and actions at convergence closely match those produced by convex relaxation. This suggests that the proposed approach reaches a solution very close to the global optimum of the original nonconvex voltage control problem. In contrast, the behavior of feedback optimization and linear control is illustrated in Fig. 1(c) and Fig. 1(d), respectively. They exhibit slow convergence and actions at convergence are far from the global optimum. Fig. 2 compares the cost function of the four methods across iterations. The cost achieved by data-driven successive linearization (red) converges to the global optimum obtained through the convex relaxation (blue). At convergence, the cost of data-driven successive linearization is 98.45% lower than that of feedback optimization and 99.64% lower than that of linear control, respectively.

To evaluate performance under different load levels, we further collect voltage and control action trajectories for 100 cases with randomly perturbed loads lasting 20 steps. Fig. 3 summarizes the mean costs over the last five steps of the trajectories under different methods. For visualization purposes, all costs are normalized using the same basis and displayed on a logarithmic y-axis. The proposed data-driven successive linearization achieves the lowest cost, with the mean value being 81.82%, 98.92%, and 99.56% lower than

those achieved by convex relaxation, feedback optimization, and linear control, respectively. Interestingly, the proposed approach can even achieve lower cost than convex relaxation. This occurs because the relaxation may not be exact when the system is lightly loaded, so the solution from convex relaxation can incur higher cost when applied to the system using the original DistFlow model. Consequently, the proposed approach consistently outperforms feedback optimization and linear control, while performing comparable or even better than the model-based voltage control approach.

B. Time Varying Load

We further evaluate the methods under time-varying load scenarios. The time-varying load is constructed using measurements of power output from an operational distribution grid [48], with additional step changes to demonstrate performance under sudden large load variations. Fig. 4 shows the voltage, reactive power, and cost trajectories over 50 time steps. The proposed data-driven successive linearization in Fig. 4(a) exhibits fast voltage recovery after each step load change. In contrast, the feedback optimization in Fig. 4(b) converges more slowly and experiences much larger voltage deviations, resulting in higher costs than successive linearization. Linear control in Fig. 4(c) exhibits the largest voltage deviations and costs, responding inefficiently to recover voltage under time-varying load. This experiment highlights the capability of successive linearization to quickly restore voltage and maintain low operational cost under dynamic load conditions.

Across 100 test cases under time-varying load conditions, Fig. 5 shows the costs achieved by different methods. Similar to the static load scenario, the cost achieved by successive linearization is lower than that achieved by feedback optimization and linear control. The mean cost of data-driven successive linearization is 44.33% and 84.89% lower than that of feedback optimization and linear control, respectively. These results demonstrate that the proposed method can adapt to a wide range of time-varying loads and efficiently recover voltage after step disturbances in net load.

VI. CONCLUSION

This paper proposes a data-driven successive linearization approach for voltage control under nonlinear power flow constraints. By conducting local linearization using Jacobian estimation from recent measurements, the method adapts to the optimization landscape of the nonconvex voltage control problem without requiring explicit power network models. Convergence guarantees to the neighborhood of KKT points are established through the design of trust-region mechanism. Numerical experiments on the IEEE 33-bus system demonstrate that the proposed approach achieves fast convergence to a low cost solution and adapts quickly to changes in net load. Directions for future work include distributed implementation under limited communication capabilities, verification on distribution systems with three-phase imbalances, and rigorous convergence analysis for systems subject to noises.

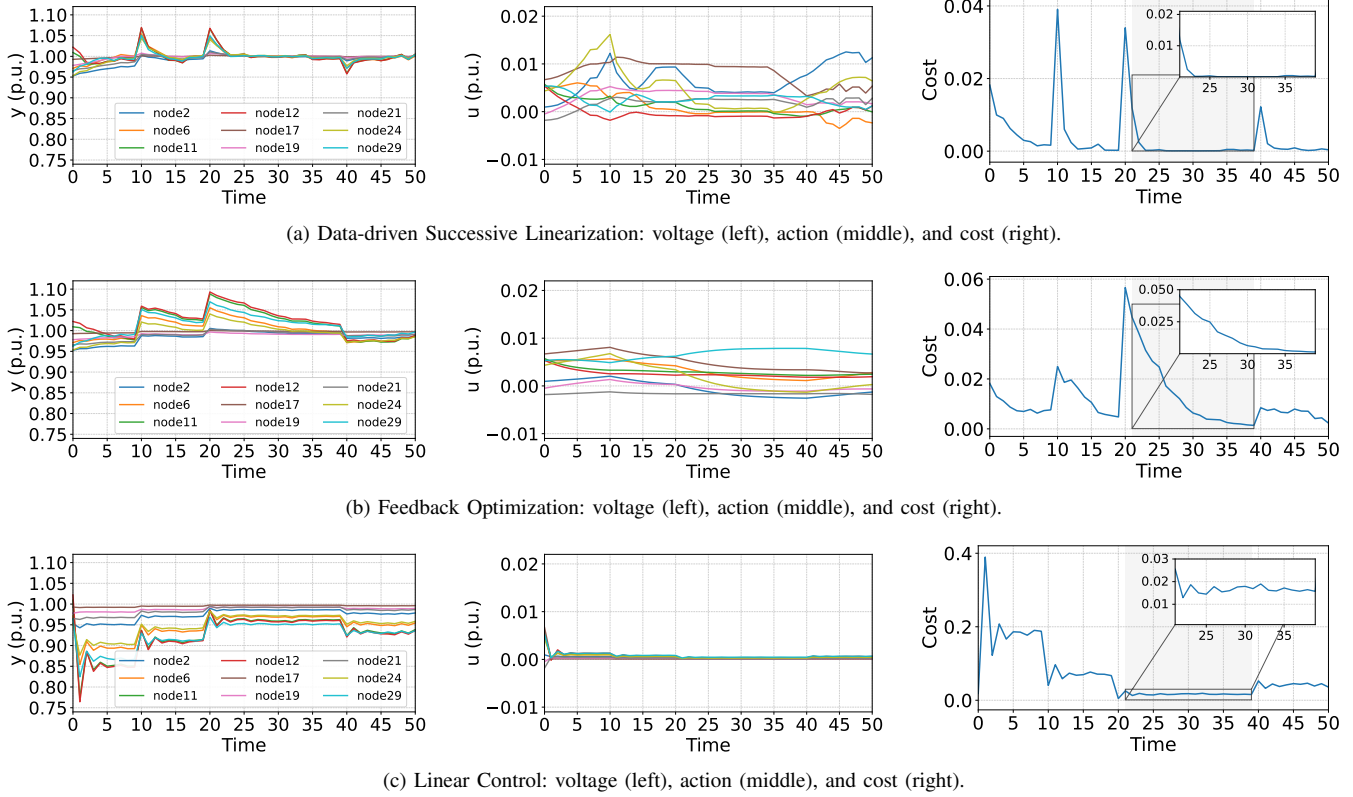


Fig. 4. Trajectories of voltage, reactive power, and cost at 9 nodes under three controllers in the time-varying load setting. Data-driven successive linearization rapidly compensates for each load change, restoring voltages close to nominal, and yielding the lowest post-disturbance cost. Feedback optimization exhibits slower recovery and a larger cost after disturbances. Linear control produces the largest voltage deviations.

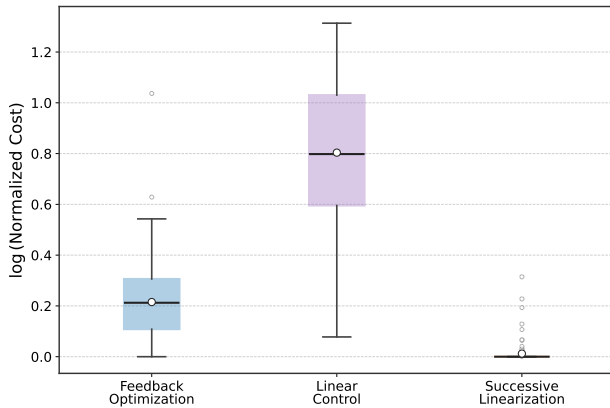


Fig. 5. Comparison of log-normalized mean costs in the time-varying load setting over 100 trials. Data-driven successive linearization attains the lowest cost, with values tightly concentrated near zero, indicating both low cost and small deviation across test cases. By contrast, feedback optimization exhibits a noticeably higher cost. Linear control performs worst with a substantially larger median and variability.

REFERENCES

- [1] K. Turitsyn, P. Sulc, S. Backhaus, and M. Chertkov, "Options for Control of Reactive Power by Distributed Photovoltaic Generators," *Proceedings of the IEEE*, vol. 99, no. 6, pp. 1063–1073, Jun. 2011. [Online]. Available: <https://ieeexplore.ieee.org/document/5768094>
- [2] H.-G. Yeh, D. F. Gayme, and S. H. Low, "Adaptive var control for distribution circuits with photovoltaic generators," *IEEE Transactions on Power Systems*, vol. 27, no. 3, pp. 1656–1663, 2012.
- [3] B. Zhang, A. Y. Lam, A. D. Domínguez-García, and D. Tse, "An optimal and distributed method for voltage regulation in power distribution systems," *IEEE Transactions on Power Systems*, vol. 30, no. 4, pp. 1714–1726, 2014.
- [4] N. Li, G. Qu, and M. Dahleh, "Real-time decentralized voltage control in distribution networks," in *2014 52nd Annual Allerton Conference on Communication, Control, and Computing (Allerton)*. IEEE, 2014, pp. 582–588.
- [5] S. Bolognani and S. Zampieri, "A distributed control strategy for reactive power compensation in smart microgrids," *IEEE Transactions on Automatic Control*, vol. 58, no. 11, pp. 2818–2833, 2013.
- [6] M. Farivar, Lijun Chen, and S. Low, "Equilibrium and dynamics of local voltage control in distribution systems," in *52nd IEEE Conference on Decision and Control*. Firenze: IEEE, Dec. 2013. [Online]. Available: <http://ieeexplore.ieee.org/document/6760555/>
- [7] H. Zhu and H. J. Liu, "Fast Local Voltage Control Under Limited Reactive Power: Optimality and Stability Analysis," *IEEE Transactions on Power Systems*, vol. 31, no. 5, pp. 3794–3803, Sep. 2016. [Online]. Available: <https://ieeexplore.ieee.org/document/7361761>
- [8] N. Li, G. Qu, and M. Dahleh, "Real-time decentralized voltage control in distribution networks," in *2014 52nd Annual Allerton Conference on Communication, Control, and Computing (Allerton)*, Sep. 2014, pp. 582–588. [Online]. Available: <https://ieeexplore.ieee.org/document/7028508>
- [9] B. Zhang, A. D. Domínguez-García, and D. Tse, "A local control approach to voltage regulation in distribution networks," in *2013 North American Power Symposium (NAPS)*, Sep. 2013, pp. 1–6. [Online]. Available: <https://ieeexplore.ieee.org/document/6666945>
- [10] W. Cui, Y. Xie, S. Low, A. Wierman, and B. Zhang, "Leveraging Predictions in Power System Voltage Control: An Adaptive Approach," Sep. 2025, arXiv:2509.09937 [eess]. [Online]. Available: <http://arxiv.org/abs/2509.09937>
- [11] N. Nazir and M. Almassalkhi, "Grid-aware aggregation and realtime disaggregation of distributed energy resources in radial networks," *IEEE Transactions on Power Systems*, vol. 37, no. 3, pp. 1706–1717, 2021.
- [12] S. Huang, Q. Wu, J. Wang, and H. Zhao, "A sufficient condition on

- convex relaxation of ac optimal power flow in distribution networks,” *IEEE Transactions on Power Systems*, vol. 32, no. 2, pp. 1359–1368, 2016.
- [13] M. Farivar and S. H. Low, “Branch flow model: Relaxations and convexification—part i,” *IEEE Transactions on Power Systems*, vol. 28, no. 3, pp. 2554–2564, 2013.
- [14] B. Zhang, A. Y. Lam, A. D. Domínguez-García, and D. Tse, “An Optimal and Distributed Method for Voltage Regulation in Power Distribution Systems,” *IEEE Transactions on Power Systems*, vol. 30, no. 4, pp. 1714–1726, Jul. 2015. [Online]. Available: <https://ieeexplore.ieee.org/document/6908041>
- [15] S. H. Low, “Convex relaxation of optimal power flow—part i: Formulations and equivalence,” *IEEE Transactions on Control of Network Systems*, vol. 1, no. 1, pp. 15–27, 2014.
- [16] —, “Convex relaxation of optimal power flow—part ii: Exactness,” *IEEE Transactions on Control of Network Systems*, vol. 1, no. 2, pp. 177–189, 2014.
- [17] Y. Chen, Y. Shi, and B. Zhang, “Data-Driven Optimal Voltage Regulation Using Input Convex Neural Networks,” *Electric Power Systems Research*, vol. 189, p. 106741, Dec. 2020. [Online]. Available: <https://www.sciencedirect.com/science/article/pii/S0378779620305447>
- [18] X. Chen, G. Qu, Y. Tang, S. Low, and N. Li, “Reinforcement learning for decision-making and control in power systems: Tutorial, review, and vision,” 2021.
- [19] C. Yeh, J. Yu, Y. Shi, and A. Wierman, “Robust online voltage control with an unknown grid topology,” in *Proceedings of the Thirteenth ACM International Conference on Future Energy Systems*, ser. e-Energy '22. New York, NY, USA: Association for Computing Machinery, Jun. 2022, pp. 240–250. [Online]. Available: <https://dl.acm.org/doi/10.1145/3538637.3538853>
- [20] J. Feng, W. Cui, J. Cortés, and Y. Shi, “Bridging Transient and Steady-State Performance in Voltage Control: A Reinforcement Learning Approach With Safe Gradient Flow,” *IEEE Control Systems Letters*, vol. 7, pp. 2845–2850, 2023. [Online]. Available: <https://ieeexplore.ieee.org/abstract/document/10163934>
- [21] Y. Shi, G. Qu, S. Low, A. Anandkumar, and A. Wierman, “Stability constrained reinforcement learning for real-time voltage control,” *American Control Conference (ACC)*, 2022.
- [22] A. D. Domínguez-García, M. Zholbaryssov, T. Amuda, and O. Ajala, “An online feedback optimization approach to voltage regulation in inverter-based power distribution networks,” in *2023 American Control Conference (ACC)*. IEEE, 2023, pp. 1868–1873.
- [23] M. Bianchi and F. Dörfler, “A stability condition for online feedback optimization without timescale separation,” *European Journal of Control*, p. 101308, 2025.
- [24] L. Ortmann, J. Maeght, P. Panciatici, F. Dörfler, and S. Bolognani, “Subtransmission grid control via online feedback optimization,” *Applied Energy*, vol. 404, p. 127142, 2026.
- [25] P. Petrov and F. Nashashibi, “Modeling and nonlinear adaptive control for autonomous vehicle overtaking,” *IEEE Transactions on Intelligent Transportation Systems*, vol. 15, no. 4, pp. 1643–1656, 2014.
- [26] J. Tordesillas, B. T. Lopez, and J. P. How, “Faster: Fast and safe trajectory planner for flights in unknown environments,” in *2019 IEEE/RSJ international conference on intelligent robots and systems (IROS)*. IEEE, 2019, pp. 1934–1940.
- [27] D. Maljuta, T. P. Reynolds, M. Szmuk, T. Lew, R. Bonalli, M. Pavone, and B. Açıkmeşe, “Convex optimization for trajectory generation: A tutorial on generating dynamically feasible trajectories reliably and efficiently,” *IEEE Control Systems Magazine*, vol. 42, no. 5, pp. 40–113, 2022.
- [28] Y. Mao, M. Szmuk, X. Xu, and B. Açıkmeşe, “Successive convexification: A superlinearly convergent algorithm for non-convex optimal control problems,” *arXiv preprint arXiv:1804.06539*, 2018.
- [29] G. Zhang and R. Mieth, “Towards reliability-aware active distribution system operations: a sequential convex programming approach: G. zhang and r. mieth,” *Optimization and Engineering*, pp. 1–47, 2025.
- [30] C. Zhao, U. Topcu, N. Li, and S. Low, “Design and stability of load-side primary frequency control in power systems,” *IEEE Transactions on Automatic Control*, vol. 59, no. 5, pp. 1177–1189, 2014.
- [31] E. Mallada, C. Zhao, and S. Low, “Optimal load-side control for frequency regulation in smart grids,” *IEEE Transactions on Automatic Control*, vol. 62, no. 12, pp. 6294–6309, Dec. 2017.
- [32] Y. Shi, B. Xu, D. Wang, and B. Zhang, “Using battery storage for peak shaving and frequency regulation: Joint optimization for superlinear gains,” *IEEE Transactions on Power Systems*, vol. 33, no. 3, pp. 2882–2894, 2017.
- [33] A. Vaccaro, G. Velotto, and A. F. Zobaa, “A decentralized and cooperative architecture for optimal voltage regulation in smart grids,” *IEEE Transactions on Industrial Electronics*, vol. 58, no. 10, pp. 4593–4602, 2011.
- [34] M. Jafari, T. O. Olowu, and A. I. Sarwat, “Optimal smart inverters voltage curve selection with a multi-objective volt-var optimization using evolutionary algorithm approach,” in *2018 North American Power Symposium (NAPS)*. IEEE, 2018, pp. 1–6.
- [35] M. E. Baran and F. F. Wu, “Optimal capacitor placement on radial distribution systems,” *IEEE Transactions on Power Delivery*, vol. 4, no. 1, pp. 725–734, 2002.
- [36] H.-D. Chiang and M. E. Baran, “On the existence and uniqueness of load flow solution for radial distribution power networks,” *IEEE Transactions on Circuits and Systems*, vol. 37, no. 3, pp. 410–416, 2002.
- [37] S. Bolognani and S. Zampieri, “On the existence and linear approximation of the power flow solution in power distribution networks,” *IEEE Transactions on Power Systems*, vol. 31, no. 1, pp. 163–172, 2015.
- [38] A. Jindal, D. Chatterjee, and R. Banavar, “Estimates of the size of the domain of the implicit function theorem: a mapping degree-based approach,” *Mathematical Control and Related Fields*, vol. 36, pp. 139–175, 2024.
- [39] B. A. Robbins and A. D. Domínguez-García, “Optimal reactive power dispatch for voltage regulation in unbalanced distribution systems,” *IEEE Transactions on Power Systems*, vol. 31, no. 4, pp. 2903–2913, 2015.
- [40] L. Ortmann, A. Hauswirth, I. Caduff, F. Dörfler, and S. Bolognani, “Experimental validation of feedback optimization in power distribution grids,” *Electric Power Systems Research*, vol. 189, p. 106782, 2020.
- [41] S. Zhan, N. G. Paterakis, W. v. d. Akker, A. van der Molen, J. Morren, and H. Slootweg, “Distributed online feedback optimization for real-time distribution system voltage regulation,” *IEEE Transactions on Power Systems*, vol. 40, no. 6, pp. 5325–5336, 2025.
- [42] S. Kinga, T. F. Megahed, H. Kanaya, and D.-E. A. Mansour, “A new voltage sensitivity-based distributed feedback online optimization for voltage control in active distribution networks,” *Computers and Electrical Engineering*, vol. 119, p. 109574, 2024.
- [43] R. Verschuere, N. van Duijkeren, R. Quirynen, and M. Diehl, “Exploiting convexity in direct optimal control: a sequential convex quadratic programming method,” in *2016 IEEE 55th Conference on Decision and Control (CDC)*. IEEE, 2016, pp. 1099–1104.
- [44] Q. T. Dinh, C. Savorgnan, and M. Diehl, “Adjoint-based predictor-corrector sequential convex programming for parametric nonlinear optimization,” *SIAM Journal on Optimization*, vol. 22, no. 4, pp. 1258–1284, 2012. [Online]. Available: <https://doi.org/10.1137/110844349>
- [45] M. E. Baran and F. F. Wu, “Network reconfiguration in distribution systems for loss reduction and load balancing,” *IEEE Power Engineering Review*, vol. 9, no. 4, pp. 101–102, 1989.
- [46] D. G. Photovoltaics and E. Storage, “Ieee standard for interconnection and interoperability of distributed energy resources with associated electric power systems interfaces,” *IEEE std*, vol. 1547, no. 1547, p. 2018, 2018.
- [47] W. Cui, Y. Xie, S. Low, A. Wierman, and B. Zhang, “Leveraging predictions in power system voltage control: An adaptive approach,” *arXiv preprint arXiv:2509.09937*, 2025.
- [48] Y. Xie, L. Werner, K. Chen, T.-L. Le, C. Ortega, and S. Low, “A digital twin of an electrical distribution grid: Social 28-bus dataset,” *arXiv preprint arXiv:2504.06588*, 2025.
- [49] R. T. Rockafellar and R. J. Wets, *Variational Analysis*, ser. Grundlehren der mathematischen Wissenschaften. Berlin, Heidelberg: Springer, 1998, hardcover published 1997-11-27; Softcover ISBN 978-3-642-08304-4 published 2010-12-01.
- [50] G. Lebourg, “Generic differentiability of lipschitzian functions,” *Transactions of the American Mathematical Society*, vol. 256, pp. 125–144, 1979.

APPENDIX

A. Proof for Lemma 1

From the trust region condition $\|z_\ell - z_k\| \leq \alpha r_k$ we obtain $\|\mathbf{u}_\ell - \mathbf{u}_k\| \leq \alpha r_k$, and therefore $\|\Delta \mathbf{u}_\ell\| \leq \|\mathbf{u}_\ell - \mathbf{u}_k\| + \|\mathbf{u}_{\ell-1} - \mathbf{u}_k\| \leq 2\alpha r_k$ on the window. As $\Delta \mathbf{y}_\ell = \mathbf{S}_\ell \Delta \mathbf{u}_\ell + \gamma_\ell$, where $\|\gamma_\ell\| \leq \beta \|\Delta \mathbf{u}_\ell\|^2$ for some constant $\beta > 0$, we can write

$$\mathbf{Y} = \mathbf{U} \mathbf{S}_k^\top + \mathbf{E}, \quad (26)$$

where

$$\mathbf{E} := \begin{bmatrix} \Delta \mathbf{u}_{k-\tau+1}^\top (\mathbf{S}_{k-\tau+1}^\top - \mathbf{S}_k^\top) + \gamma_{k-\tau+1}^\top \\ \vdots \\ \Delta \mathbf{u}_k^\top (\mathbf{S}_k^\top - \mathbf{S}_k^\top) + \gamma_k^\top \end{bmatrix}.$$

For the weighted least-squares problem, the estimator satisfies $\tilde{\mathbf{S}}_k^\top = (\mathbf{U}^\top \mathbf{W} \mathbf{U})^{-1} \mathbf{U}^\top \mathbf{W} \mathbf{Y}$, where $\mathbf{W} \in \mathbb{R}^{\tau \times \tau}$ is the diagonal weight matrix defined in (7). Substituting (26) into this expression yields

$$\tilde{\mathbf{S}}_k^\top - \mathbf{S}_k^\top = (\mathbf{U}^\top \mathbf{W} \mathbf{U})^{-1} \mathbf{U}^\top \mathbf{W} \mathbf{E}. \quad (27)$$

Note that when the operating point is not near the voltage-collapse boundary, the Jacobian $\nabla_{\mathbf{u}} \mathbf{g}(\mathbf{u})$ is locally Lipschitz. Denote the local Lipschitz constant of Jacobian as L_S . We have $\|\mathbf{S}_\ell - \mathbf{S}_k\| \leq L_S \|\mathbf{u}_\ell - \mathbf{u}_k\| \leq L_S \alpha r_k$; together with $\|\Delta \mathbf{u}_\ell\| \leq 2\alpha r_k$, this implies $\|\Delta \mathbf{u}_\ell^\top (\mathbf{S}_\ell^\top - \mathbf{S}_k^\top)\| \leq \|\Delta \mathbf{u}_\ell\| \|\mathbf{S}_\ell - \mathbf{S}_k\| \leq (2\alpha r_k)(L_S \alpha r_k) = 2L_S \alpha^2 r_k^2$. Moreover, from the remainder bound $\|\gamma_\ell\| \leq c \|\Delta \mathbf{u}_\ell\|^2$, we obtain $\|\gamma_\ell\| \leq c(2\alpha r_k)^2 = 4c\alpha^2 r_k^2$. Hence each row of \mathbf{E} has norm at most $2L_S \alpha^2 r_k^2 + 4c\alpha^2 r_k^2 \leq c'_E r_k^2$ for some constant $c'_E > 0$, and therefore $\|\mathbf{E}\|_F^2 \leq \tau (c'_E)^2 r_k^4$, so $\|\mathbf{E}\|_F \leq \sqrt{\tau} c'_E r_k^2 \leq c_E r_k^2$ for some constant $c_E > 0$. In particular, $\|\mathbf{E}\| \leq \|\mathbf{E}\|_F \leq c_E r_k^2$. Also,

$$\|\mathbf{U}\| \leq \|\mathbf{U}\|_F \leq \left(\sum_{\ell=k-\tau+1}^k \|\Delta \mathbf{u}_\ell\|^2 \right)^{1/2} \leq 2\alpha \sqrt{\tau} r_k.$$

Consequently, $\|\mathbf{U}^\top \mathbf{W}\| \leq \|\mathbf{W}\| \|\mathbf{U}\| \leq c_U r_k$ for some constant $c_U > 0$.

Under the sufficient excitation condition 1, there exists $m > 0$ such that $\sigma_{\min}(\mathbf{U}) \geq m r_k$. Since \mathbf{W} is positive definite, there exists $w_{\min} > 0$ with $\lambda_{\min}(\mathbf{W}) \geq w_{\min}$, so $\lambda_{\min}(\mathbf{U}^\top \mathbf{W} \mathbf{U}) \geq w_{\min} \sigma_{\min}^2(\mathbf{U}) \geq w_{\min} m^2 r_k^2$. Hence

$$\|(\mathbf{U}^\top \mathbf{W} \mathbf{U})^{-1}\| = \frac{1}{\lambda_{\min}(\mathbf{U}^\top \mathbf{W} \mathbf{U})} \leq \frac{1}{w_{\min} m^2 r_k^2},$$

where $\lambda_{\min}(\cdot)$ denotes the smallest eigenvalue and $\sigma_{\min}(\cdot)$ denotes the smallest singular value. Therefore, from (27),

$$\begin{aligned} \|\tilde{\mathbf{S}}_k - \mathbf{S}_k\| &\leq \|(\mathbf{U}^\top \mathbf{W} \mathbf{U})^{-1}\| \|\mathbf{U}^\top \mathbf{W}\| \|\mathbf{E}\| \\ &\leq \frac{1}{w_{\min} m^2 r_k^2} (c_U r_k) (c_E r_k^2) = \frac{c_U c_E}{w_{\min} m^2} r_k. \end{aligned} \quad (28)$$

Consequently, for any $\|z - z_k\| \leq r_k$,

$$\|(\tilde{\mathbf{S}}_k - \mathbf{S}_k)(\mathbf{u} - \mathbf{u}_k)\| \leq \frac{c_U c_E}{w_{\min} m^2} r_k \cdot r_k = o(r_k),$$

which proves (15).

B. Proof for Lemma 5

Since \bar{z} is feasible and not stationary, $\mathbf{0} \notin \partial J(\bar{z})$. According to the definition of the generalized differential, $\partial J(\bar{z})$ is a closed convex set; hence, by the separating hyperplane theorem to $\partial J(\bar{z})$ and the origin, there exist a unit vector \mathbf{s} and a constant $\kappa > 0$ such that $\varphi^\top \mathbf{s} \leq -\kappa$ for all $\varphi \in \partial J(\bar{z})$. Thus, by the upper semicontinuity of Clarke's directional derivative, we have

$$\limsup_{\substack{z \rightarrow \bar{z} \\ r \rightarrow 0}} \frac{J(z + r\mathbf{s}) - J(z)}{r} \leq -\kappa,$$

which implies that there exists $\bar{\epsilon} > 0$ and $\bar{r} > 0$ for which

$$J(z + r\mathbf{s}) - J(z) \leq -\frac{\kappa}{2} r \quad \forall z \in N(\bar{z}, \bar{\epsilon}), \forall r \in (0, \bar{r}]. \quad (29)$$

For any k with $z_k \in N(\bar{z}, \bar{\epsilon})$ and any $r_k \in (0, \bar{r}]$. Consider the trial step $\mathbf{d}'_k := r_k \mathbf{s}$, which locates within the trust region of \bar{r} since $\|\mathbf{d}'_k\| = r_k$. Evaluating (29) at $z = z_k$ and $r = r_k$ gives

$$\Delta J_k(z_k, \mathbf{d}'_k) := J(z_k) - J(z_k + \mathbf{d}'_k) \geq \frac{\kappa}{2} r_k. \quad (30)$$

By Lemma 3, for all \mathbf{d} with $\|\mathbf{d}\| \leq r_k$, $J(z_k + \mathbf{d}) - \tilde{L}_k(\mathbf{d}) = o(r_k)$. Applying this with $\mathbf{d} = \mathbf{d}'_k$ and rearranging yields

$$\begin{aligned} \Delta \tilde{L}_k(z_k, \mathbf{d}'_k) &= J(z_k) - \tilde{L}_k(\mathbf{d}'_k) \\ &= \Delta J_k(z_k, \mathbf{d}'_k) + o(r_k) \\ &\geq \frac{\kappa}{2} r_k + o(r_k). \end{aligned} \quad (31)$$

Because \mathbf{d}_k^* minimizes \tilde{L}_k over $\{\mathbf{d} : \|\mathbf{d}\| \leq r_k\}$,

$$\Delta \tilde{L}_k(z_k, \mathbf{d}_k^*) \geq \Delta \tilde{L}_k(z_k, \mathbf{d}'_k) \geq \frac{\kappa}{2} r_k + o(r_k). \quad (32)$$

Again by Lemma 3, evaluating (19) at $\mathbf{d} = \mathbf{d}_k^*$ and subtracting from $J(z_k)$ gives

$$\begin{aligned} \Delta J_k(z_k, \mathbf{d}_k^*) &= J(z_k) - J(z_k + \mathbf{d}_k^*) \\ &= J(z_k) - \tilde{L}_k(\mathbf{d}_k^*) - o(r_k) \\ &= \Delta \tilde{L}_k(z_k, \mathbf{d}_k^*) - o(r_k). \end{aligned} \quad (33)$$

Dividing (33) by (32) yields

$$\rho(z_k, r_k) = \frac{\Delta J_k(z_k, \mathbf{d}_k^*)}{\Delta \tilde{L}_k(z_k, \mathbf{d}_k^*)} \geq 1 - \frac{o(r_k)}{(\kappa/2) r_k + o(r_k)}.$$

This completes the proof.

C. Proof for Lemma 6

Since the constraint set is compact, the sequence $\{z_k\}$ admits a convergent subsequence by the Bolzano–Weierstrass theorem. Let $\{z_{k_i}\}$ be any such subsequence with $z_{k_i} \rightarrow \bar{z}$. Define the subsequence Jacobian mismatch level

$$\bar{\epsilon} := \liminf_{i \rightarrow \infty} \|\tilde{\mathbf{S}}_{k_i} - \mathbf{S}_{k_i}\|.$$

By the definition of the lower limit, there exists a subsequence such that $\|\tilde{\mathbf{S}}_{k_i} - \mathbf{S}_{k_i}\| \rightarrow \bar{\epsilon}$. We could still denote this subsequence by $\{k_i\}$ for simplicity.

Assume, for contradiction, that \bar{z} lies outside the neighborhood of the stationary set of J , namely $\text{dist}(\mathbf{0}, \partial J(\bar{z})) > \|\boldsymbol{\lambda}\| \bar{\epsilon}$. In particular, $\mathbf{0} \notin \partial J(\bar{z})$. Since J is locally Lipschitz,

$\partial J(\bar{z})$ is a nonempty closed convex set. Let s' be the projection of $\mathbf{0}$ onto $\partial J(\bar{z})$, so $\|s'\| = \text{dist}(\mathbf{0}, \partial J(\bar{z}))$ and $s' \neq \mathbf{0}$. Set $s := -s'/\|s'\|$, so $\|s\| = 1$. By the projection variational inequality, for all $\varphi \in \partial J(\bar{z})$, $(\varphi - s')^\top (\mathbf{0} - s') \leq 0$, from which we have

$$\varphi^\top s \leq -\|s'\| = -\text{dist}(\mathbf{0}, \partial J(\bar{z})) \quad \forall \varphi \in \partial J(\bar{z}). \quad (34)$$

By outer semicontinuity of the Clarke subdifferential [49], there exists $\epsilon_1 > 0$ such that for all $z \in N(\bar{z}, \epsilon_1)$ and $\varphi \in \partial J(z)$,

$$\varphi^\top s \leq -\left(\text{dist}(\mathbf{0}, \partial J(\bar{z})) - \frac{\delta}{4}\right), \quad (35)$$

where we take $\delta := \text{dist}(\mathbf{0}, \partial J(\bar{z})) - \|\lambda\| \bar{e} > 0$.

Let $\epsilon'_1 := \epsilon_1/2$. For any $z \in N(\bar{z}, \epsilon'_1)$ and any $r \in (0, \epsilon'_1]$, the segment $\{z + trs : t \in [0, 1]\}$ is contained in $N(\bar{z}, \epsilon_1)$. By Lebourg's mean value theorem for locally Lipschitz functions [50], there exist $t \in (0, 1)$ and $\varphi \in \partial J(z + trs)$ such that $J(z + rs) - J(z) = r\varphi^\top s$. Combining this with (35) yields

$$J(z + rs) - J(z) \leq -\left(\text{dist}(\mathbf{0}, \partial J(\bar{z})) - \frac{\delta}{4}\right)r, \quad (36)$$

$$\forall z \in N(\bar{z}, \epsilon'_1), \forall r \in (0, \epsilon'_1].$$

By Lemma 5, there exist $\epsilon_2 > 0$ and $\bar{r} > 0$ such that for every k_i with $z_{k_i} \in N(\bar{z}, \epsilon_2)$ and every radius $r_{k_i} \in (0, \bar{r}]$, any optimal solution $\mathbf{d}_{k_i}^*$ of the trust-region subproblem at z_{k_i} satisfies

$$\frac{\Delta J_{k_i}(z_{k_i}, \mathbf{d}_{k_i}^*)}{\Delta \tilde{L}_{k_i}(z_{k_i}, \mathbf{d}_{k_i}^*)} \geq \rho_0 > 0, \quad (37)$$

where ρ_0 is a positive constant number. Without loss of generality, assume each z_{k_i} in the subsequence locates within $N(\bar{z}, \bar{e})$ with $\bar{e} = \min\{\epsilon'_1, \epsilon_2\}$, and the trust-region radius r_k satisfies $0 < \underline{r} \leq r_k \leq \bar{r}$ for all k .

Next, fix a constant step length $\hat{r} > 0$ satisfying

$$\hat{r} \leq \min\{\underline{r}, \epsilon'_1\}.$$

Then $\|\hat{r}s\| = \hat{r} \leq r_{k_i}$, so the trial step $\mathbf{d}'_{k_i} := \hat{r}s$ is feasible for every trust region along the subsequence. Since $\|\tilde{\mathbf{S}}_{k_i} - \mathbf{S}_{k_i}\| \rightarrow \bar{e}$, there exists i_0 such that, for all $i \geq i_0$,

$$\|\tilde{\mathbf{S}}_{k_i} - \mathbf{S}_{k_i}\| \leq \bar{e} + \frac{\delta}{4\|\lambda\|}. \quad (38)$$

Define

$$\begin{aligned} \theta &:= \liminf_{i \rightarrow \infty} \Delta \tilde{L}_{k_i}(z_{k_i}, \mathbf{d}_{k_i}^*) \\ &= \liminf_{i \rightarrow \infty} \left(J(z_{k_i}) - \tilde{L}_{k_i}(\mathbf{d}_{k_i}^*) \right). \end{aligned} \quad (39)$$

By Lemma 4, $\Delta \tilde{L}_{k_i}(z_{k_i}, \mathbf{d}_{k_i}^*) \geq 0$ for all i , hence $\theta \geq 0$. We now show that $\theta > 0$. Fix $i \geq i_0$. As $z_{k_i} \in N(\bar{z}, \bar{e})$, evaluating (36) at $z = z_{k_i}$ and $r = \hat{r}$ gives

$$\begin{aligned} \Delta J_{k_i}(z_{k_i}, \mathbf{d}'_{k_i}) &= J(z_{k_i}) - J(z_{k_i} + \mathbf{d}'_{k_i}) \\ &\geq \left(\text{dist}(\mathbf{0}, \partial J(\bar{z})) - \frac{\delta}{4}\right)\hat{r}. \end{aligned} \quad (40)$$

To relate $J(z_{k_i} + \mathbf{d}'_{k_i})$ and $\tilde{L}_{k_i}(\mathbf{d}'_{k_i})$, write

$$\begin{aligned} J(z_{k_i} + \mathbf{d}'_{k_i}) - \tilde{L}_{k_i}(\mathbf{d}'_{k_i}) &= \left(J(z_{k_i} + \mathbf{d}'_{k_i}) - L_{k_i}(\mathbf{d}'_{k_i}) \right) \\ &\quad + \left(L_{k_i}(\mathbf{d}'_{k_i}) - \tilde{L}_{k_i}(\mathbf{d}'_{k_i}) \right). \end{aligned} \quad (41)$$

By Lemma 2, there exists $r_0 > 0$ such that for all $\|\mathbf{d}\| \leq r_0$, $|J(z_{k_i} + \mathbf{d}) - L_{k_i}(\mathbf{d})| \leq \frac{\delta}{4}\|\mathbf{d}\|$. Take $\hat{r} \leq r_0$, so this applies to $\mathbf{d} = \mathbf{d}'_{k_i}$ and yields

$$\left| J(z_{k_i} + \mathbf{d}'_{k_i}) - L_{k_i}(\mathbf{d}'_{k_i}) \right| \leq \frac{\delta}{4}\hat{r}.$$

Since $\phi_{\mathbf{M}}(\mathbf{d}) = \lambda^\top |\mathbf{d}_y - \mathbf{M}\mathbf{d}_u|$ is Lipschitz in \mathbf{M} ,

$$\begin{aligned} \left| L_{k_i}(\mathbf{d}'_{k_i}) - \tilde{L}_{k_i}(\mathbf{d}'_{k_i}) \right| &= \left| \phi_{\mathbf{S}_{k_i}}(\mathbf{d}'_{k_i}) - \phi_{\tilde{\mathbf{S}}_{k_i}}(\mathbf{d}'_{k_i}) \right| \\ &\leq \|\lambda\| \|\tilde{\mathbf{S}}_{k_i} - \mathbf{S}_{k_i}\| \|\mathbf{d}'_{k_i}\| \\ &\leq \left(\|\lambda\| \bar{e} + \frac{\delta}{4} \right) \hat{r}, \end{aligned} \quad (42)$$

where the last line uses (38). Now, use $\Delta \tilde{L}_{k_i}(z_{k_i}, \mathbf{d}'_{k_i}) = \Delta J_{k_i}(z_{k_i}, \mathbf{d}'_{k_i}) + \left(J(z_{k_i} + \mathbf{d}'_{k_i}) - \tilde{L}_{k_i}(\mathbf{d}'_{k_i}) \right)$, together with (40), (41), and the bounds above, to obtain

$$\begin{aligned} \Delta \tilde{L}_{k_i}(z_{k_i}, \mathbf{d}'_{k_i}) &\geq \left(\text{dist}(\mathbf{0}, \partial J(\bar{z})) - \frac{\delta}{4}\right)\hat{r} \\ &\quad - \frac{\delta}{4}\hat{r} - \left(\|\lambda\| \bar{e} + \frac{\delta}{4}\right)\hat{r} \\ &= \left(\text{dist}(\mathbf{0}, \partial J(\bar{z})) - \|\lambda\| \bar{e} - \frac{3\delta}{4}\right)\hat{r} \\ &= \frac{\delta}{4}\hat{r} > 0. \end{aligned} \quad (43)$$

Since $\mathbf{d}_{k_i}^*$ minimizes \tilde{L}_{k_i} over $\{\mathbf{d} : \|\mathbf{d}\| \leq r_{k_i}\}$, we have $\Delta \tilde{L}_{k_i}(z_{k_i}, \mathbf{d}_{k_i}^*) \geq \Delta \tilde{L}_{k_i}(z_{k_i}, \mathbf{d}'_{k_i}) \geq \frac{\delta}{4}\hat{r}$. Taking lower limit yields $\theta \geq \frac{\delta}{4}\hat{r} > 0$, hence $\theta > 0$.

By the definition of θ in (39) and $\theta > 0$, there exists i_2 such that for all $i \geq i_2$, $\Delta \tilde{L}_{k_i}(z_{k_i}, \mathbf{d}_{k_i}^*) \geq \theta/2 > 0$. Since $z_{k_i} \in N(\bar{z}, \bar{e})$ and $r_{k_i} \in (0, \bar{r}]$, the lower bound (37) applies; therefore,

$$\begin{aligned} J(z_{k_i}) - J(z_{k_{i+1}}) &= \Delta J_{k_i}(z_{k_i}, \mathbf{d}_{k_i}^*) \\ &\geq \rho_0 \Delta \tilde{L}_{k_i}(z_{k_i}, \mathbf{d}_{k_i}^*) \\ &\geq \rho_0 \theta/2 > 0, \end{aligned} \quad (44)$$

where the first equality uses the update $z_{k_{i+1}} = z_{k_i} + \mathbf{d}_{k_i}^*$. From (44), we obtain $J(z_{k_{i+1}}) \leq J(z_{k_i})$ holds for all k . As $k_i + 1 \leq k_{i+1}$, we have $J(z_{k_{i+1}}) \geq J(z_{k_{i+1}})$. Hence, for any $N \geq i_2$, $\sum_{i=i_2}^N (J(z_{k_i}) - J(z_{k_{i+1}})) \leq J(z_{k_{i_2}}) - J(z_{k_{N+1}})$. Letting $N \rightarrow \infty$ and using $z_{k_i} \rightarrow \bar{z}$ yields

$$\sum_{i=i_2}^{\infty} (J(z_{k_i}) - J(z_{k_{i+1}})) \leq J(z_{k_{i_2}}) - J(\bar{z}) < \infty.$$

Therefore the series on the left converges, and necessarily $J(z_{k_i}) - J(z_{k_{i+1}}) \rightarrow 0$, which contradicts the uniform lower bound (44). Consequently, the contradiction assumption is false. Thus,

$$\text{dist}(\mathbf{0}, \partial J(\bar{z})) \leq \|\lambda\| \liminf_{i \rightarrow \infty} \|\tilde{\mathbf{S}}_{k_i} - \mathbf{S}_{k_i}\|.$$

Equivalently, \bar{z} is $\|\lambda\| \liminf_{i \rightarrow \infty} \|\tilde{\mathbf{S}}_{k_i} - \mathbf{S}_{k_i}\|$ -close to the stationary set \mathcal{T} of the penalty problem (10).